Combined CFD – Numerical Integration Method for the Determination of Exterior Ballistics for a Reactive Projectile

Ovidiu IORGA, Mihail MUNTEANU, Marius MĂRMUREANU,
Viorel ȚIGĂNESCU, and Alexandru MARIN

***Abstract*—The present paper presents both experimental and simulation conducted results in case of a thermobaric projectile for SPG-9 recoilless rifle, caliber 73 mm. The simulation consists in determining main forces such as aerodynamic drag, lift, and other parameters like the center of pressure, the center of mass and inertial moments, etc. On the other hand, the experimental results consisted of performing a series of firing, with real and inert rocket engines, during which the velocity of the projectile was measured. The values obtained were subsequently used to validate the numerical simulation.**

***Index Terms*—CFD simulation, drag and lift coefficients, thermobaric projectile, velocity.**

I. Introduction

For a new projectile, calculations have to be made in order to determine different parameters necessary for conducting the firing. This paper aims to present a method for evaluating the variation of velocity and for determining the trajectory of a new projectile (given the angle of firing), by using CFD simulations (here implemented in SolidWork's Flow simulation module) and numerical integration (using Matlab). This approach simplifies the determination of coefficients that classic literature usually either refers to tabulated data, or requires a significant number of experimental firings. The results from the simulation are compared to data extracted from real firings in order to validate the method. All the simulations and firings are made for a piercing thermobaric projectile for SPG-9 recoilless rifle, caliber 73 *mm*.

"This work was supported by a grant of the Ministry of Research, Inovation and digitization, CNCS/CCCDI - UEFISCDI, project number PN-III-P2-2.1-PTE-2019-0256, within PNCDI III".

O. Iorga is chemical engineer and PhD candidate at the Doctoral School of Military Technical Academy "Ferdinand I" in Bucharest in the domain mechanical engineering. Currently he is researcher at Scientific Research Center for CBRN Defense and Ecology, in Bucharest, Romania (email: ovidiu.iorga@nbce.ro).

M. Munteanu is junior scientific researcher at Scientific Research Center for CBRN Defense and Ecology, Bucharest, Romania and PhD candidate at Military Technical Academy "Ferdinand I" in Bucharest (email: mihail.munteanu@nbce.ro).

M. Mărmureanu is senior researcher and Ph.D. în mechanical engineering. Currently he holds the position of head of laboratory whitin Miltary Equipment and Technologies Research Agency from Clinceni, Romania (email: mărmureanu_marius@yahoo.com).

V. T. Țigănescu is professor at Military Technical Academy "Ferdinand I" in Bucharest and general director of the Miltary Equipment and Technologies Research Agency from Clinceni, Romania (email: viorel.tiganescu@mta.ro).

A. Marin is junior scientific researcher at Scientific Research Center for CBRN Defense and Ecology, Bucharest, Romania and PhD candidate at Military Technical Academy "Ferdinand I" in Bucharest (email: mihail.munteanu@nbce.ro).

II. Simulation and Numerical Calculus

The movement of an unguided reactive projectile is described in respect to the coordinate system $O_p x_p y_p z_p$, which is bound to the earth, the origin, O_p being situated at the extremity of the launcher. The "earth bound" system has its $O_p x_p$ axis oriented according to the direction of the horizontal of the firing plane (the vertical plane that contains the axis of the launcher) in the direction of the movement, the axis $O_p y_{p\,p}$ – according to the local vertical, and the $O_p z_p$ axis, after a lateral horizontal direction. In the center of mass of the projectile, *O*, we consider the system $O_p X_p Y_p Z_p$ having the axes parallel to the $Ox_p y_p z_p$ system. This system only makes a translation movement with velocity $\vec{V}$ of the center of mass.

The coordinate system "linked to velocity" *OXYZ* can be obtained by three rotations: θ_0 – launching angle, ψ_L – negative rotation, and θ_L (Fig. 1) [2-3]:

$$OX_p Y_p Z_p \xrightarrow[OZ_p \equiv OZ_L]{\theta_0} OX_L Y_L Z_L \xrightarrow[OY_L \equiv OY'_L]{\psi_L} OX'_L Y'_L Z'_L \xrightarrow[OZ'_L \equiv OZ]{\theta_L} OXYZ \quad (1)$$

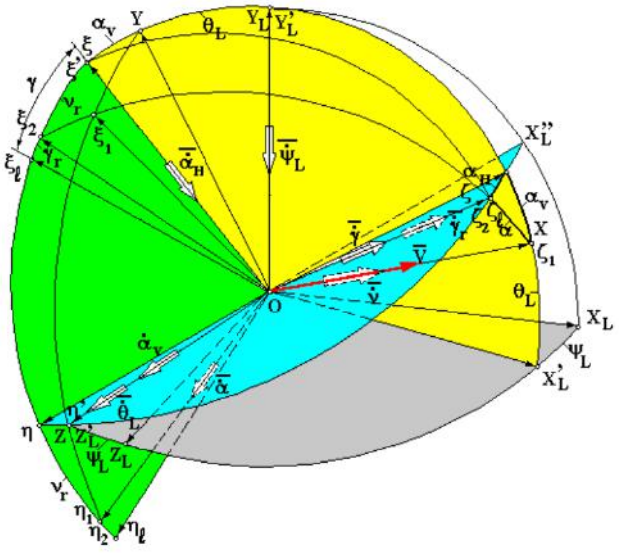

Figure 1. Coordinate system rotation [2]

The projectile body position relative to the reference frame linked to velocity can be determined by three consecutive rotations of α_V, α_H and γ angles:

$$OXYZ \xrightarrow[OZ\equiv O\eta']{\alpha_V} O\xi'\eta'\zeta' \xrightarrow[O\xi'\equiv O\xi]{\alpha_H} O\xi\eta\zeta \xrightarrow[O\zeta\equiv O\zeta_\ell]{\gamma} O\xi_\ell\eta_\ell\zeta_\ell \tag{2}$$

The projectile body position may be also defined by the following rotations: ν (precession angle), α (incidence angle) and γ_r (angle of a proper rotation nature):

$$OXYZ \xrightarrow[OX\equiv O\zeta_1]{\nu} O\xi_1\eta_1\zeta_1 \xrightarrow[O\eta_1\equiv O\eta_2]{\alpha} O\xi_2\eta_2\zeta_2 \xrightarrow[O\zeta_2\equiv O\zeta_\ell]{\gamma_r} O\xi_\ell\eta_\ell\zeta_\ell \tag{3}$$

The movement of the projectile is determined if at any moment the following parameters are known: V, ψ_L, θ_L, α_H, α_V and γ.

In order to write the equations of motion for the unguided reactive projectile, the following forces and moments in relation to the center of mass are considered:

- *the thrust force*, in the opposite direction to the $O\xi$ axis;
- *the drag force*, in the opposite direction to the OX axis;
- *the lift force*, along the $O\xi_1$ axis;
- *the additional lift force*, which occurs due to the pitch movement, called by some authors [4] pitch force – along the $O\xi_1$ axis;
- *the gravity force*, in the opposite direction to the OY axis;
- *the main aerodynamic moment*, including the effects of transverse aerodynamic damping along the $O\eta_2$ axis;
- *the spin damping moment*;
- *the jet damping moment*.

Based on the above, considering an unguided reactive projectile with slow rotational motion having the center of mass in front of the center of pressure, the forces are projected on the axes of the velocity related system ($OXYZ$), and the moments on the axes of the system $O\xi\eta\zeta$ and, developing the terms, the general equations of motion are obtained as follows:

- movement of the center of mass [2-3]:

$$\frac{dV}{dt} = \frac{1}{m}\left[T\cos\alpha_V\cos\alpha_H - \frac{\rho V^2}{2}SC_x - mg\left(\sin\theta_0\cos\theta_L\cos\psi_L + \cos\theta_0\sin\theta_L\right)\right] \tag{4}$$

$$\frac{d\theta_L}{dt} = \frac{1}{mV}\left[T\sin\alpha_V\cos\alpha_H + \frac{\rho V^2}{2}SC_Z^\alpha\left(\alpha + \frac{l_c\omega_{\eta 2}}{V}\right)\cos\nu - mg\left(\cos\theta_0\cos\theta_L - \sin\theta_0\sin\theta_L\cos\psi_L\right)\right] \tag{5}$$

$$\frac{d\psi_L}{dt} = \frac{1}{mV\cos\theta_L}\left[T\sin\alpha_H + \frac{\rho V^2}{2}SC_Z^\alpha\left(\alpha + \frac{l_c\omega_{\eta 2}}{V}\right)\sin\nu + mg\sin\theta_0\sin\psi_L\right] \tag{6}$$

- movement around the center of mass [5]:

$$\frac{d\omega_\xi}{dt} = \frac{1}{J}\left\{-\left(J_\zeta - J\right)\omega_\eta\omega_\zeta - J\omega_\eta\frac{d\gamma}{dt} + \frac{\rho V^2}{2}SC_x\cos\alpha_V\sin\alpha_H l_c + \frac{\rho V^2}{2}SC_Z^\alpha\left(\alpha + \frac{l_c\omega_{\eta 2}}{V}\right)\left(\cos\alpha_H\sin\nu - \sin\alpha_V\sin\alpha_H\cos\nu\right)l_c - \left[\frac{dJ}{dt} + \left|\frac{dm}{dt}\right|\left(z_e^2 + \frac{1}{4}R_e^2\right)\right]\omega_\xi\right\} \tag{7}$$

$$\frac{d\omega_\eta}{dt} = \frac{1}{J}\left\{-\left(J - J_\zeta\right)\omega_\xi\omega_\zeta + J\omega_\xi\frac{d\gamma}{dt} - \frac{\rho V^2}{2}SC_x\sin\alpha_V l_c - \frac{\rho V^2}{2}SC_Z^\alpha\left(\alpha + \frac{l_c\omega_{\eta 2}}{V}\right)\cos\alpha_V\cos\nu l_c - \left[\frac{dJ}{dt} + \left|\frac{dm}{dt}\right|\left(z_e^2 + \frac{1}{4}R_e^2\right)\right]\omega_\eta\right\} \tag{8}$$

$$\frac{d\omega_\eta}{dt} = -\frac{1}{J_\zeta}\left(\frac{\rho V}{S}Sl_r^2C_{ax} + \frac{dJ_\zeta}{dt} + \frac{1}{2}\left|\frac{dm}{dt}\right|R_e^2\right)\omega_\zeta \tag{9}$$

- kinematic equations between angular velocities [2-3]:

$$\frac{d\alpha_V}{dt} = \frac{\omega_\eta}{\cos\alpha_H} - \frac{d\theta_L}{dt} - \sin\left(\theta_L + \alpha_V\right)\mathrm{tg}\alpha_H\frac{d\psi_L}{dt} \tag{10}$$

$$\frac{d\alpha_H}{dt} = -\omega_\xi - \cos\left(\theta_L + \alpha_V\right)\frac{d\psi_L}{dt} \tag{11}$$

$$\frac{d\gamma}{dt} = \omega_\zeta - \mathrm{tg}\alpha_H\omega_\eta + \frac{\sin\left(\theta_L + \alpha_V\right)}{\cos\alpha_H}\frac{d\psi_L}{dt} \tag{12}$$

- expressions for the coordinates of the center of mass [2-3]:

$$\frac{dx}{dt} = V\left(\cos\theta_0\cos\theta_L\cos\psi_L - \sin\theta_0\sin\theta_L\right) \tag{13}$$

$$\frac{dy}{dt} = V\left(\sin\theta_0\cos\theta_L\cos\psi_L + \cos\theta_0\sin\theta_L\right) \tag{14}$$

$$\frac{dz}{dt} = V\cos\theta_L\sin\psi_L \tag{15}$$

- additional relations for the precession angle ν, the nutation angle α and the angular velocity $\omega_{\eta 2}$ are [5]:

$$\nu = \mathrm{arctg}\left(\frac{\mathrm{tg}\alpha_H}{\sin\alpha_V}\right) \tag{16}$$

$$\alpha = \mathrm{sgn}\left(\alpha_V\right)\arccos\left(\cos\alpha_V\cos\alpha_H\right) \tag{17}$$

$$\omega_{\eta 2} = -\cos\alpha_V\sin\nu\omega_\xi + \frac{\cos\nu}{\cos\alpha_H}\omega_\eta \tag{18}$$

The system of equation used to evaluate the above mentioned parameters is the classical one, and can be found in detailed form in references [1-2,6]. The equations were solved by numerical integration using MatLab. Fig. 2 presents the functional diagram of the program used.

 Digital Object Identifier 10.32754/JMT.2021.1.01

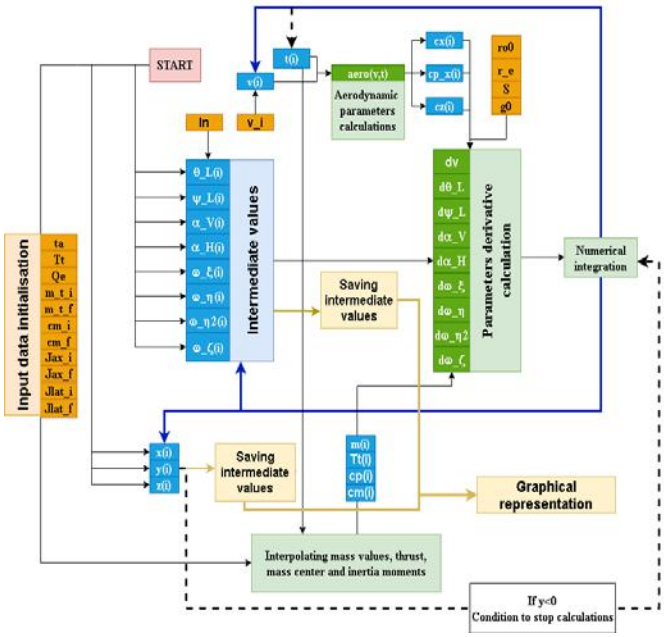

Figure 2. The diagram of the program used in MatLab for calculating the exterior ballistic parameters

In Fig. 2 in *orange* are represented the input data, as detailed in Table I.

TABLE I. DETAILS REGARDING THE INPUT DATA

Input data	Detailed parameter	Value	Unit
ta	rocket motor burning time	0.4	[*s*]
Tt	thrust	2700	[*N*]
cm_i	mass center position (before launch)	247	[*mm*]
cm_f	mass center position (after burning of rocket motor)	227	[*mm*]
Jax_i	axial longitudinal moment of inertia (before launch)	3.503×10^{-3}	[$kg\cdot m^2$]
Jax_f	axial longitudinal moment of inertia (after burning of rocket engine)	3.363×10^{-3}	[$kg\cdot m^2$]
Jlat_i	axial transversal moment of inertia (before launch)	0.127162	[$kg\cdot m^2$]
Jlat_f	axial transversal moment of inertia (after burning of rocket engine)	0.149996	[$kg\cdot m^2$]
m_t_i	mass of projectile before launch	5500	[*g*]
m_t_f	mass of projectile after burning of rocket engine	5030	[*g*]
In	launch angle	0-3	[*deg*]
v_i	initial velocity	270	[*m/s*]
ro0	air density in standard conditions	1.225	[kg/m^3]
r_e	exit radius of rocket nozzle	12.5	[mm^2]
S	maximum transversal area	4183	[mm^2]
g0	gravitational acceleration	9.81	[m/s^2]

In *blue*, there are the intermediate values computed by the program on each iteration:

V – velocity
T – physical time elapsed
cx – position of center of mass
cp_x – position of center of pressure (measured from the front of the projectile)
cz – lift coefficient derivative in respect to the angle of attack
x – position along *X* axis
y – position along *Y* axis
z – position along *Z* axis
m – mass

In *green*, functions (subprograms) that are called at each iteration.

Beside the set of input data presented, there is another set contained in the functions that determine the aerodynamic forces (drag, lift). These are determined by running CFD simulations on the 3D model. For the drag, lift and center of pressure, the simulations were performed using a computational domain of 1300×500×500 *mm*, consisting of 302701 cells. The basic mesh is presented in Fig. 3, but the cells presented here are further refined when the simulation is started near the solid-fluid interface.

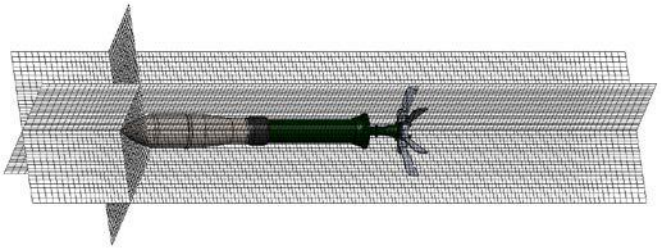

Figure 3. Basic mesh used for determining main aerodynamic parameters

The main forces determined by simulation were performed in the following manner:

1. The aerodynamic drag

To evaluate the aerodynamic drag, the simulation was set to a steady state simulation, in an atmosphere of air (taken from the SolidWorks library of materials). The thermal exchange between the model and the fluid was ignored (adiabatic). The surface roughness was set to 3.2 μm (this was considered as the experimental shots fired were not painted, leaving the surface as it was after the machining operations). A set of simulations were performed, varying the velocity of the fluid by increments of 20 *m/s*, from 200 to 430 *m/s*.

An approach using a time-dependent simulation was first tried, though the time span necessary for the convergence of the set of values that were meant to be extracted (drag and lift, in this case) was too wide to be neglected, or any relevant data to be extracted.

While still remaining at this subject, an important factor for the time necessary for the simulation (except the well known parameters, such as the number of cells or the tolerance for convergence) is usually the "freeze" option. This option (set to periodical) calculates all the values taken into account for a number of given iterations, and then sets the variables that are usually known for fast convergence to the last computed value, while trying to "keep up" with the rest. This option, however, does not really improve time of simulation in our case, for the global goals (force, in our case) are dependent on the "frozen" values.

2. The lift (used for later determining the lift coefficient derivative in respect to the angle of attack)

In the first approach, the time dependent simulation was attempted once again. An inlet was set (velocity type), as big as the whole boundary of the computational domain in the transversal plane, and keeping its velocity constant along the longitudinal axis and changing the value of the velocity along the *Y* axis, in a few steps, as to vary the angle of attack from 0 to 0.71°. While at first this approach seemed to provide promising results, the simulation did not behave in the expected matter. For example, Fig. 4 shows the values

obtained from a time-dependent simulation run by varying the velocity along the *Y* axis in a periodic manner (0; 0.5; 1; 1.5; 2; 2.5 m/s) and the velocity along the *X* axis in the range 200–400 *m*/*s*. As it can be observed, as the time of the simulation (or the number of iterations) increases, the results start to be filled with noise, without converging to a clear step, as in the first five steps. Additionally, the results for zero angle of attack tend to get further from zero, a result that for the ideal conditions of the simulation makes no sense. For a symmetrical shape, in a flow distributed symmetrically around the longitudinal axis, given a small turbulence, a force different than zero along the *Y* axis may be acceptable, but the values obtained, which tend to be (at their maximum) 23% of the value of lift for an angle of attack of 0.43°, are unacceptable. This can be seen clearly in Fig. 4 (lower graph), the zero value on the vertical axis being marked with a red line. Each data series corresponds to a set of values determined for the lift force on different angles made by fluid velocity to the model, but given the maximum values obtained (~10 *N*) for the 300 *m*/*s* series at 0.43°, the value obtained for 0° (~2 *N*) presents too much of an error. Hence, the simulations were finally performed individually for each angle and velocity.

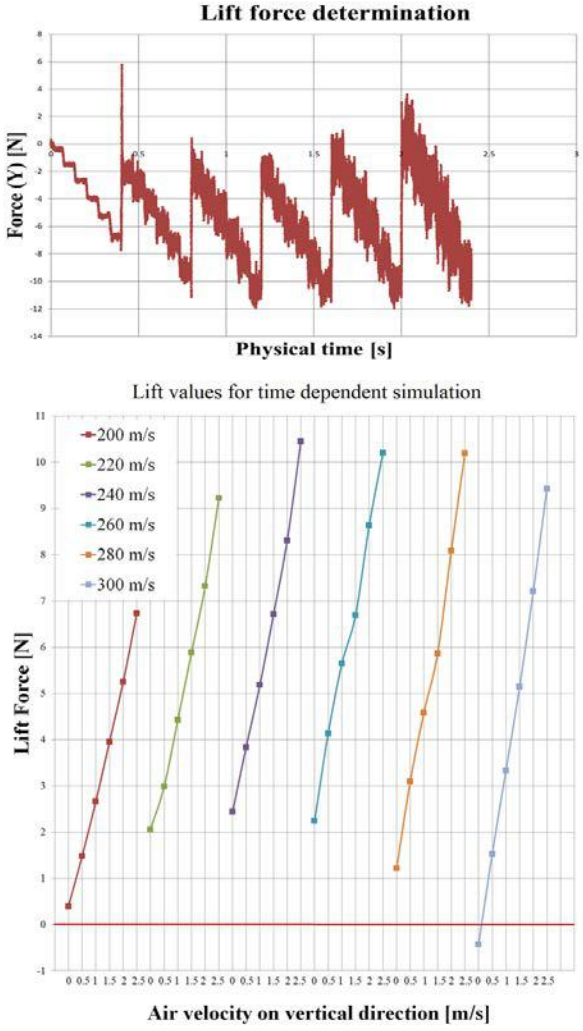

Figure 4. Lift force determination from a time-dependent simulation

3. The center of mass and moments of inertia

These values were straightforward to determine and their variation in respect to time, given the fact that the values were obtained from evaluating the 3D model and given the relatively linear law for the mass loss rate.

4. The center of pressure

The variation of the center of pressure turned out to be the most complicated to determine of all. Not because of its definition, but because there is no software implementation or easy method for determining the law of variation. There are a few simplified methods that can be used to calculate it. The easiest of all methods is determining the center of mass for the profile (outline) of the model. This, however, does not account for bodies (or parts) that are not the result of a revolution around a longitudinal axis. Another method requires the computation of the area of all the sections of the projectile that can be represented as simple shapes, and then compute a weighted mean by considering the areas and the distance from a given point for every center of given areas. This gives a better approximation, since, for example, one can take into account surfaces as the stabilizing fins (and the number of fins), but does not reflect the reality since it does not take into account the distribution of pressure along the projectile.

In order to obtain the variation, we returned to the CFD simulation. The projectile was split into 20 surfaces (Fig. 5) along the longitudinal axis, and then again each of the 6 stabilizing fins into 2 opposing surfaces. Then, simulations were performed for different values of the fluid velocity and the center of pressure computed by inserting an equation goal, following a numerical integration expression for the pressure distribution. The resulting variation is presented in Fig. 5.

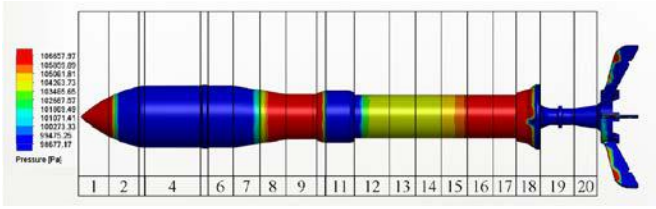

Figure 5. The surfaces selected for pressure goals in the flow simulation, used in determining the center of pressure

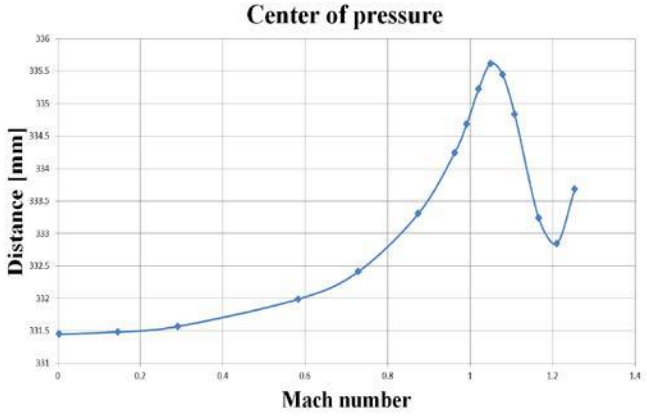

Figure 6. Center of pressure distance from the tip of the projectile

The ratio l_c/l_r (l_c – *distance between center of pressure and center of mass*, l_r – *length of the projectile*), representing the coefficient of static stability or the stability reserve, must range between 10% and 20% (if it is too high, the undirected reactive projectile becomes vulnerable to the action of the wind). In our case, minimum and maximum values of center of pressure vary between 12% and 16%.

5. The thrust

The thrust turned out to be a force that necessitated a few considerations in order to obtain it using CFD simulation. A few attempts were made, until settling on one value. In the

 Digital Object Identifier 10.32754/JMT.2021.1.01

first tried out simulation, the whole model was used, with a more or less uniform mesh (which turned out to be a very poor choice, given the size of the throat area of the nozzle in respect to the whole projectile, and even more so, in respect to the whole computational domain). The next approach used only the body of the rocket engine and the nozzle in order to reduce the size and simplify the whole assembly. The following parameters greatly influence thrust calculation:

5.1 The position of the inlet. One of the first attempts to determine the thrust was made by setting the end face of the rocket engine interior as inlet. This seemed to render all results unusable, since the momentum of gasses leaving the selected face was transferred by the Flow simulation module to the body of the rocket engine itself, thus altering the obtained value.

5.2 The composition of the fluid. In order to obtain close to reality results, the mix of gasses should also be the closest as it can be to the real exhaust gasses. This influences the results by means of specific volume, density, and sound velocity. All of these values are strongly influenced by the mean molar mass of the mix.

5.3 The temperature of the gasses. Besides the percentage of components in the fluid, the initial temperature influences the other parameters (density, sound velocity, etc.).

5.4 The size of the computational domain. Setting the computational domain too short on the longitudinal axis, so that the exhaust does not fully expand and reach its limit velocity, greatly influences the results obtained. A short domain will render the results completely unrealistic, as probably the software integrates the forces over a domain where the values of pressure and velocity jump abruptly from those in the exhaust to those of a normal atmosphere (at the boundary of the computational domain).

Given these considerations, the inlet was set as a mass rate flow (one of the only variables obtained using experimental data, as the mass of the propellant was known and the time of burning was measured using high-speed video and doppler radar recordings) by using the whole cylindrical inner face of the rocket engine, so that the momentum of the entering gasses into the domain are cancelled. The flow rate was set at 1.17 *kg*/*s*. The final computational domain was set to 2600 *mm* in length, shown in Fig. 7, as to cover the whole expansion of gasses, given the exhaust velocity contour. The composition of the gasses was defined as a mix of CO_2 (13%), CO (62%, user defined material), H_2O (13%) and N_2 (12%), all percentages as weight fractions, and the temperature was set to 1800 *K* as an approximation for the propellant (PRTF-200) [7].

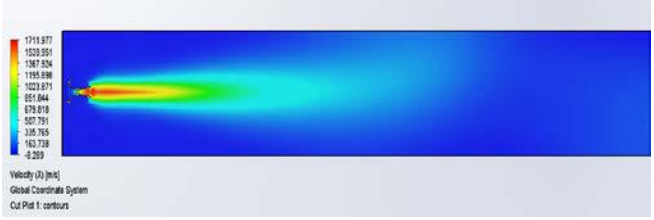

Figure 7. A cut plot of the velocity of gasses passing through and escaping the nozzle

All these values were either entered in the MatLab program as input data (thrust), or further processed in order to obtain the coefficient of drag, lift, or for interpolation of the center of pressure.

Two plots representing the velocity variation and trajectory (for a 1.8 degree firing angle) are shown in Fig. 8.

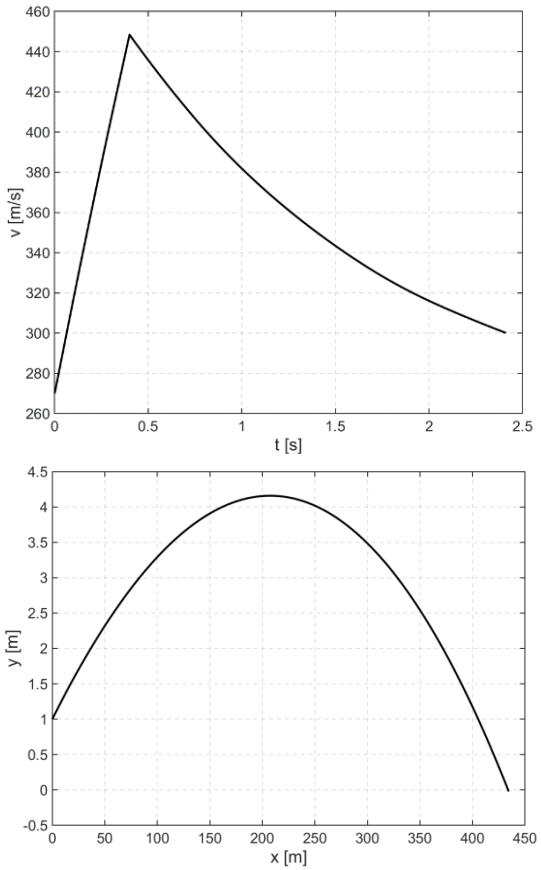

Figure 8. Velocity vs time (upper) and trajectory (lower) plots from numerical simulation

III. Experimental Research

A series of real firings was conducted. The velocity of the projectile was measured using a Doppler radar (Fig. 9), with a flame detector used as a trigger for the beginning of the measurement. Both real and inert rocket engines were used in the experimental ammunition.

Figure 9. The launcher in firing position with the Doppler radar placed near the barrel and a projectile ready to be loaded

The data ilustrated by the velocity-time curves (Fig. 10) correspond to the complete trajectory of the projectile between the muzzle and the target impact moment (placed at 200 m distance). The closest accurate and relevant velocities that can be measured may be considered from $t = 30\ ms$, whereas values before this moment are without physical relevance. Until 100 ms, there could still be observed irrelevant scattered points on the graph (noise), caused by

gasses and small particles expelled from the bore with the projectile. These values were ignored in the data sets when the graphs were made. However, the program in MatLab does not compute the first part of the trajectory, before the rocket engine starts, so for those recordings this part is not of much interest. It can serve however to determine clearly the initial velocity.

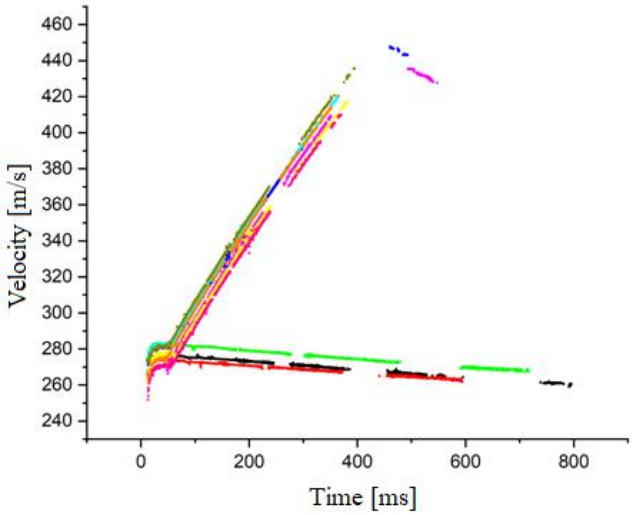

Figure 10. Velocity data obtained from Doppler radar measurements

These values were used in comparison to the one obtained by numerical simulations, as to validate the model. Fig. 11 shows the two sets of data superimposed, both for real engine rocket and inert rocket engine.

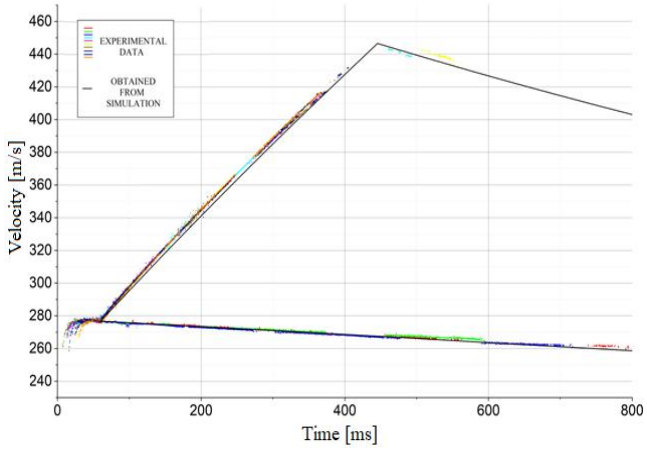

Figure 11. Superimposed results from simulation and data from Doppler *radar*

Using this model, we can now predict velocities and determine the distance the projectile reaches (as well as remaining velocity) for every given angle within a very reasonable margin of error. Fig. 12 presents a series of trajectories plotted for different angles. For all these trajectories, it was taken the initial height of the barrel of 1 m.

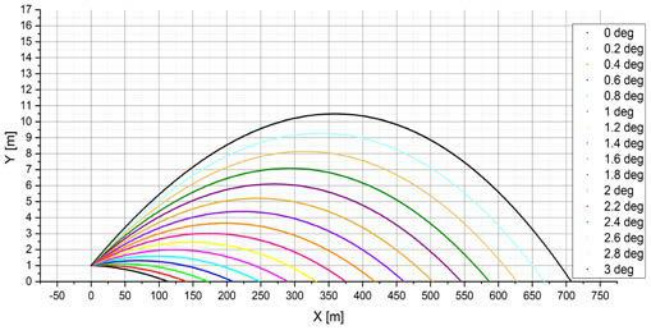

Figure 12. Trajectories plotted for a series of launch angles

IV. Conclusion

The method presented here is suitable for obtaining the aerodynamical parameters needed in order to solve, by means of numerical integration, the equations of motion for an unguided reactive projectile. The time-velocity data obtained were compared to the experimental recordings. The main aerodynamical forces can be reliably obtained by means of numerical simulations, but great attention must be directed to the mesh size and positioning of inlets (in case of thrust determination), and the composition of exhaust gasses must also be well known. Steady state simulations, conducted in steps of velocity/angle of incidence are suited for the purpose and can be used to obtain the variance curves for drag and lift coefficients.

Acknowledgement

The authors would like to thank senior researcher Constantin Puica, from Military Equipment and Technologies Research Agency for providing support in the numerical simulation, including the software and hardware resources.

References

[1] F. Moraru, *Exterior ballistics manual*, Military Publishing House, Bucharest, 1976 (in Romanian).

[2] Fl. Moraru, *On the ecuations of the general movement of a rocket in a resistive medium. Studies and research of applied mechanics*, R.S.R. Academy Publishing House, Nr. 4, Tom 31, 1972, pp. 753-779 (in Romanian).

[3] F. Moraru, D. Safta and L. Moraru, *Mathematical Model for the Rocket General Motion Simulation in Presence of Various Perturbations*. Proceedings of the 4th Conference on Weapons Systems, Brno, 4-6 May 1999, pp. 66-81.

[4] M.-M. Niță and D.-St. Andreescu, *Unguided and guided rocket flight*. Military Publishing House, Bucharest, 1964 (in Romanian).

[5] M. I. Mărmureanu, *Research regarding flow in rocket nozzle and consequences to rocket flight dynamics, PhD thesis*, Polytechnic University of Bucharest, 2014 (in Romanian).

[6] P. Șomoiag, C.-E. Moldoveanu, H. Daudé and P. Ferrier, *Particularities of Ballistic Performances for Unguided Rockets.* Proceedings of the 19th International Conference – The Knowledge-Based Organization, KBO June 2013, Sibiu.

[7] O. Dumitru and P. Emanoil, *Interior ballistics of rocket engines. Military Academy*, Bucharest, 1971 (in Romanian).

 Digital Object Identifier 10.32754/JMT.2021.1.01